Effect of Biaxial Strain on SnO_2 Bandgap: First-Principles Calculations

Zineb Kerrami, Anass Sibari, Marwan Lakhal,
Abdelilah Benyoussef and Mohammed Benaissa*
LMPHE, Department of Physics,
Faculty of Sciences, University Mohammed V
Rabat, Morocco
* benaissa.um5@gmail.com

Omar Mounkachi*, Mohammed Hamedoun and
Abdelilah Benyoussef
Institute of Nanomaterial's and Nanotechnology
MAScIR
Rabat, Morocco
* o.mounkachi@mascir.com

Abdelilah Benyoussef
Hassan II Academy of Science and Technology
Rabat, Morocco

Abstract— **In the present study, the variation of the band gap energy with biaxial strain in SnO_2 in its bulk form is examined using state-of-the-art first-principles calculations. All calculations were based on DFT within the Tran-Blaha modified Becke-Johnson exchange potential approximation (TB-mBJ). Under biaxial compressive and tensile strain, the projected densities of states showed that valence and conduction bands blue- and red-shift respectively. Hybrid oxygen and tin conduction states were shown to provide covalent bonding interaction which directly affects the band gap. In the case of a tensile strain, a decrease of the charge distribution around tin sites is observed which elongates the Sn-O bond and decreases the band gap energy. However, an opposite behavior is demonstrated in the case of compression which clearly demonstrates the ability of strain to modulate the band structure. Finally, our results suggest that the SnO2 structure is very flexible and by mechanical strain we can efficiently modulate its electronic properties and band gap to improve its suitability for optoelectronic and thermoelectric applications.**

Keywords- SnO2; Biaxial Strain; Density Functional Theory; Band Structure Modulation.

I. INTRODUCTION

Strain-engineering of semiconductor band-edge structure is a major approach to advance devices with enhanced carrier mobility, such as field-effect transistors (FETs) [1,2], laser diodes (LDs) with reduced lasing threshold and gain [3], wavelength-tuning of optoelectronic devices including solar-cells [4,5], and nano-piezotronics of piezoelectric materials [6]. Therein, band-edge parameters, such as bandgap Eg, are tuned by strain. In the field of transparent conductive oxide (TCO) semiconductors, bandgap engineering as a function of size has also been studied. In the case of tin dioxide (SnO2), theoretical studies have shown that Eg can be tuned which is a promising way to widen its application in photovoltaics, for instance, due to its low resistivity, high transmittance, and stronger mechanical and chemical stability than other oxides [7,8]. However, its wide band gap of 3.6 eV, which is large compared with the visible light energy, is limiting its integration into photovoltaic devices. One way of overcoming such an obstacle, several studies have shown that external pressure and internal strain effects can be conducted where interatomic potential (atomic distances and bonds) variation should have a direct impact on the band structure. For example, different experimental and theoretical studies have shown that the strain and stress can be used to control the band gap of TiO2 [9,10,11], ZnO [12], MgO and CdO [13]. In addition, it has been reported that tensile strain induced by the mis-match between SnO2 thin film deposited on a sapphire (Al2O3) substrate has a significant impact on structural parameters and optical band gap of SnO2 [14]. This finding motivated us to examine the variation of the band gap energy with biaxial strain in SnO2 in its bulk form by performing state-of-the-art first-principles calculations.

II. COMPUTATIONAL DETAILS

In this article, all calculations were performed with the Wien2k package [15] based on the density functional theory (DFT) using the Full Potential Linearized Augmented Plane-Wave (FP-LAPW) method. The exchange correlation potential was evaluated using the Generalized Gradient Approximation (GGA) by Perdew, Burk, and Ernzerhof (GGA-PBE) [16] to optimize the volume and the internal position parameters, although it is well known that the band gap is severely underestimated for many semiconductors and insulators using LDA or GGA. So we propose in this work the Tran-Blaha modified Becke-Johnson (TB-mBJ) [17] optimization to improve the band gap calculation. The self-consistent calculations are considered to be convergent only when the calculated total energy of the crystal converges to less than 0.01×10^{-3} Ry, obtained by 500 k-points in the irreducible symmetry wedge of the first Brillouin zone. The bulk SnO_2 crystallizes in the rutile-type structure (space group P42/mnm). The lattice coordinates of a Sn atom position is located at (0,0,0) and the two O atoms positions are located at (u,u,0), where u=0.3056 [18]. The equilibrium lattice constants used as input in the calculation are obtained from our GGA-PBE calculations, such as: $a_0 = b_0 = 4.76$ Å and $c_0 = 3.29$ Å, as illustrated in Fig.1a. Under biaxial strain, ***a*** and ***b*** lattice constants were given different but fixed values in order to simulate either a compression or a tension, while the relaxation of the crystal is freely performed along the ***c*** axis for each ***a***(***b***) given values. In this figure case, the biaxial strain can be expressed as:

$$\varepsilon_{xx}(\%) = \varepsilon_{yy}(\%) = (a(b)-a_0(b_0))/a_0(b_0). \quad (1)$$

III. RESULTS AND DISCUSSIONS

We then considered a series of biaxial strain values ranging from -6% to +6% imposed in the ***ab*** plane, where negative strain values represent a compressive strain while positive ones represent a tensile strain. Fig.1b shows the variation of the ***c*** lattice parameter and its corresponding unit-cell volume under different values of $\varepsilon_{xx}(\varepsilon_{yy})$. As can be seen, the ***c*** lattice parameter increases under biaxial compressive strain and shrinks under biaxial tensile strain, whereas, SnO_2 unit-cell volume increases or decreases linearly as a function of the strain percent. Thus we can conclude that the ***c*** lattice parameter variation shows a relatively weak ability to maintain the crystal volume constant when the ***ab*** plane is distorted causing therefore a structural deformation of the SnO_2 unit-cell.

Fig.2 shows the calculated band structure of SnO_2 under various strain values along high symmetry directions of the Brillouin zone. In the present calculation, the valence band maximum (VBM) is set equal to $E-E_F = 0$, where E_F is the Fermi level energy. It is noticed from the band structure that the VBM and the conduction band minimum (CBM) occur at the Γ point, which clearly demonstrates that SnO_2 remains a direct band gap semiconductor under strain, a fact that is of immense benefit to photonic and optoelectronic applications since optical transitions can be maintained in the absence of phonons contribution [19,20]. The calculated band gap of unstrained SnO_2 is 3.593 eV, a value that is close to the experimental one [14], *i.e.* 3.6 eV. From Fig.2, we can clearly notice that the band gap decreases under tensile strain, but increases under compressive strain.

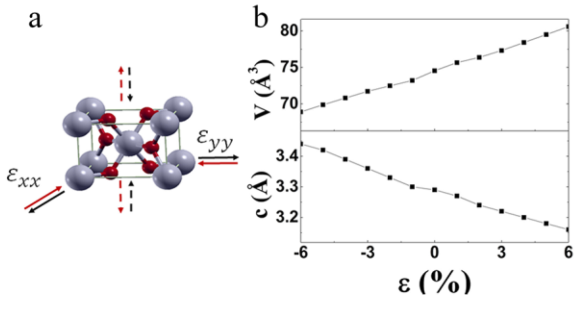

Figure 1. SnO_2 Unit Cell Structure (a). The Sn, and O Atoms Are Represented by Gray, And Red Spheres Respectively. Red-Solid and Black-Solid Arrows Present The Compressive and Tensile Strain Respectively. Dashed Arrows Indicates The ***c*** Lattice Movement Under Compressive (Red) and Tensile Strain (Black)**.** Calculation of The ***c*** Lattice Parameter (b) and Its Corresponding Unit-Cell Volume Under Strain.

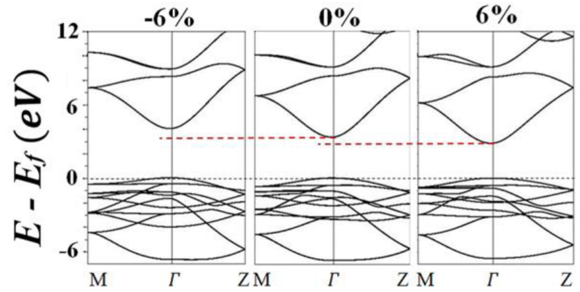

Figure 2. Calculated Band Structure of SnO2 Under Three Strain Values. The Dashed Red Lines Show The Shift of The CBM as a Function Of Strain.

The projected densities of states (DOS) of strained and unstrained SnO_2 are presented in Fig.3. In general, under compressive and tensile strain, valence and conduction bands seem to blue- and red-shift respectively. In addition, the blue-shift of the conduction band (CB) is higher than that of the valence band (VB). This progressive increase of the CB leads to a significant increase of the band gap energy. However, analogical description can be undertaken in the case of a tensile strain where a progressive and rapid decrease of the CB seems to lead to a band gap reduction. In each case, the valence band width either expands or retracts depending on the strain value demonstrating again the efficiency of an applied strain to provoke a motion of the energy band structure. First, it is seen that the VB is mainly composed of O-2p states and admixture of Sn-4p,d states, whereas the CB is formed by O-2p and Sn-5s states hybridization, the nature of which does not change under biaxial strain (tensile or compressive).

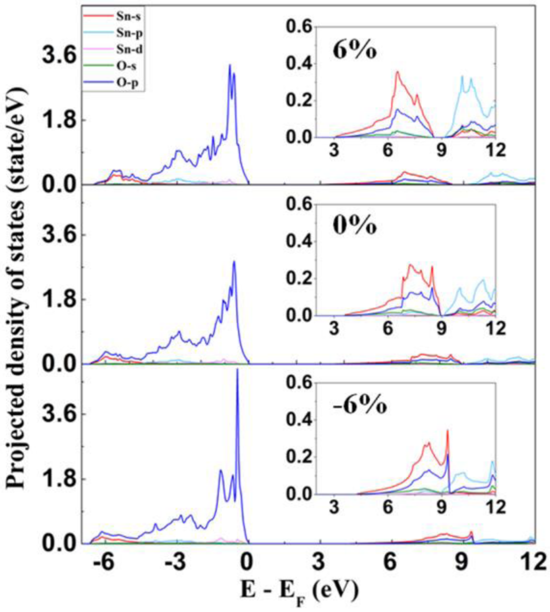

Figure 3. Calculated Projected Density of States Of Strained and Unstrained SnO2. The Inset Shows a Zoom on The CB.

Second, this hybridization provides covalent bonding interaction between Sn and O. Indeed, the band gap reflects directly the strength of the covalent bond; stronger the covalent interaction is, wider is the band gap. A better picture of these effects is illustrated in the charge density distributions, shown in Fig.4, viewed along the [110] axis. We can notice that an increase in the compressive strain is accompanied with an increase of the charge distribution around Sn sites due to a charge transfer from O to Sn. In addition, the Sn-O bond becomes shorter (stronger) which increases the charge density induced by this shrunk volume, and then explains the band gap energy increase. Again, an opposite behavior is demonstrated in the case of a tensile biaxial strain.

To further appreciate the strain effect on the band gap, we examine the variation of the VBM and CBM energies with strain, as plotted in Fig.5. These energies decrease with expansion and increase with compression. In addition, the slope of the CBM plot is slightly smaller (i.e. more negative) than that of the VBM plot. This results in a nearly linear behavior of the band gap (inset). Consequently, the band gap energy undergoes a clear modulation under biaxial strain varying from 4.42 to 3.08 eV as the strain value varies from -6% to +6%, respectively, which is in agreement with reported experimental and theoretical studies [21,22]. It is therefore concluded that the band gap of SnO_2 can be effectively modulated by lattice strain which may also benefit to other important applications in the field of optoelectronic and thermoelectric efficiency [23,24,25].

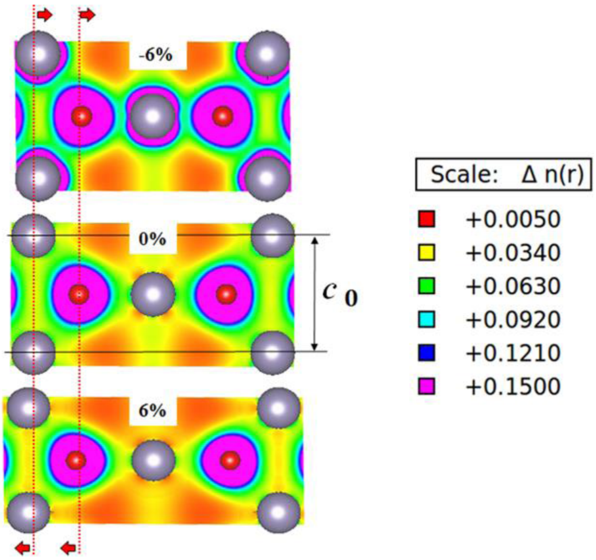

Figure 4. Calculated Charge Density Distribution in The (110) Plane of Strained and Unstrained SnO2. Red and Grey Balls Are O and Sn Atoms Respectively. The Red Dashed Lines and Arrows Display The Sn and O Atoms Position Under Strain and The Deformation Direction. The Thermoscale Represents The Charge Concentration Per Area (eÅ^{-2}).

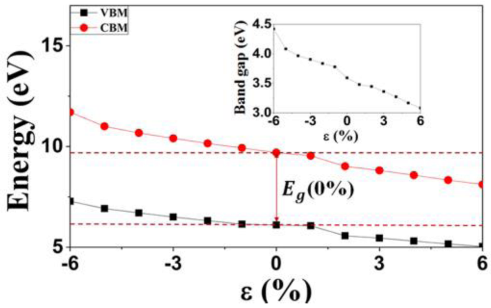

Figure 5. Calculation of The Valence Band Maximum (VBM) and Conduction Band Minimum (CBM) Under Strain, The Inset Is The Calculated Band Gap Energy of SnO2 as Function of Strain.

IV. CONCLUSION

In conclusion, we have studied theoretically the effect of biaxial strain on SnO2 properties using first-principles calculations. Our DOS and charge distribution calculations showed, on one hand, that the valence band width either expands or retracts depending on the strain value demonstrating the efficiency of an applied strain to provoke a motion of the energy band structure. Due to a tensile strain, on the other hand, a weakening of the O-p and Sn-s hybridization in the conduction band is obtained because of less charge transfer from O to Sn atoms causing therefore a band gap energy modulation.

REFERENCES

[1] J. Bardeen, W. Shockley, “Deformation potentials and mobilities in non-polar crystals,” Phys. Rev. Vol. 80, p. 72 (1950).

[2] Y. M. Niquet, C. Delerue, C. Krzeminski, “Effects of strain on the carrier mobility in silicon nanowires,” Nano Lett. Vol. 12, pp. 3545-3550 (1950).

[3] M. Silver, E. Reilly, “Gain and radiative current density in InGaAs/lnGaAsP lasers with electrostatically confined electron states,” IEEE J. Quantum Electron. Vol. 30, pp. 547-553 (1994).

[4] G. Signorello, S. Karg, M. T. Björk, B.Gotsmann, H.Riel, “Tuning the light emission from GaAs nanowires over 290 meV with uniaxial strain,” Nano Lett. Vol. 13, pp. 917-924 (2013).

[5] J.Feng, X. Qian, C. W. Huang, and J. Li, “Strain-engineered artificial atom as a broad-spectrum solar energy funnel,” Nature Photon. Vol. 6, pp. 866-872 (2012).

[6] Z. L. Wang, “Nanopiezotronics,” Adv. Mater. Vol. 19, pp. 889-892 (2007).

[7] O. Mounkachi, E. Salmani, M. Lakhal, et al. “Band-gap engineering of SnO2,” Sol. Energ. Mat. Sol. Cells. Vol. 148, pp. 34-38 (2016).

[8] T. Fukano, T. Motohiro, T. Ida, and H. Hashizume, “Ionization potentials of transparent conductive indium tin oxide films covered with a single layer of fluorine-doped tin oxide nanoparticles grown by spray pyrolysis deposition,” J. Appl. Phys. Vol. 97, p. 084314 (2005).

[9] L. Thulin, J. Guerra, « Calculations of strain-modified anatase TiO2 band structures,” Phys. Rev.B. Vol. 77, p. 195112 (2008).

[10] V. Swamy, A. Y. Kuznetsov, L. S. Dubrovinsky, A.Kurnosov, V. B. Prakapenka, “Unusual compression behavior of anatase TiO2 nanocrystals,” Phys. Rev. Lett. Vol. 103, p. 075505 (2009).

[11] W. J. Yin, S. Chen, J. H. Yang, et al. “Effective band gap narrowing of anatase TiO2 by strain along a soft crystal direction,” Appl. Phys. Lett. Vol. 96, p. 221901 (2010).

[12] S. Yadav, T. Sadowski, and R. Ramprasad, "Density functional theory study of Zn X (X= O, S, Se, Te) under uniaxial strain," Phys. Rev. B. Vol. 81, p. 144120 (2010).

[13] Q. Yan, P. Rinke, M. Winkelnkemper, et al. "Strain effects and band parameters in MgO, ZnO, and CdO," Appl. Phys. Lett. Vol. 101, p. 152105 (2012).

[14] W. Zhou, Y. Liu, Y. Yang, and P. Wu, "Band gap engineering of SnO2 by epitaxial strain: experimental and theoretical investigations," J. Phys. Chem. C. Vol. 118, pp. 6448-6453 (2014).

[15] P. Blaha, K. Schwarz, G. K. H. Madsen, et al. & Luitz, J. wien2k. An augmented plane wave+ local orbitals program for calculating crystal properties. (2001).

[16] J. P. Perdew, K. Burke, and M. Ernzerhof, "Generalized gradient approximation made simple," Phys. Rev. lett. Vol. 77, p. 3865 (1996).

[17] F. Tran, and P. Blaha, "Accurate band gaps of semiconductors and insulators with a semilocal exchange-correlation potential," Phys. Rev. Lett. Vol. 102, p. 226401 (2009).

[18] A. A. Bolzan, C. Fong, B. J. Kennedy, and C. J. Howard, "Structural studies of rutile-type metal dioxides," Acta Crystallogr., Sect. B: Struct. Sci. Vol. 53, pp. 373-380 (1997).

[19] B. Amin, I. Ahmad, M. Maqbool, S. Goumri-Said, and R. Ahmad, "Ab initio study of the bandgap engineering of Al1− xGaxN for optoelectronic applications," J. Appl. Phys. Vol. 109, p. 023109 (2011).

[20] B. Amin, I. Ahmad, M. Maqbool, "Conversion of direct to indirect bandgap and optical response of B substituted InN for novel optical devices applications," J. Lightwave Technol. Vol. 28, pp. 223-227 (2010).

[21] K. Bakht, T. Mahmood, M. Ahmed, and K. Abid, "Pressure induced electronic and optical properties of rutile SnO 2 by first principle calculations," Superlattices Microstruct. Vol. 90, pp. 236-241 (2016).

[22] S. Tingting, Z. Fuchun, and Z. Weihu, "Density Functional Theory Study on the Electronic Structure and Optical Properties of SnO2," Rare Metal Mat. Eng. Vol. 44, pp. 2409-2414 (2015).

[23] H. Wang, Z. M. Gibbs, Y. Takagiwa, and G. J. Snyder, "Tuning bands of PbSe for better thermoelectric efficiency," Energy Environ. Sci. Vol. 7, pp. 804-811 (2014).

[24] R. C. Picu, T. Borca-Tasciuc, and M. C. Pavel, "Strain and size effects on heat transport in nanostructures," J. Appl. Phys. Vol. 93, pp. 3535-3539 (2003).

[25] A. R. Abramson, C. L. Tien, and A. Majumdar, "Interface and strain effects on the thermal conductivity of heterostructures: a molecular dynamics study," J. Heat Transfer. Vol. 124, pp. 963-970 (2002).